frontiers | Frontiers in Materials

TYPE Original Research
PUBLISHED 18 September 2023
DOI 10.3389/fmats.2023.1264529

OPEN ACCESS

EDITED BY
Arun Prabhu Rameshbabu,
Harvard Medical School, United States

REVIEWED BY
Barnali dasgupta Ghosh,
Birla Institute of Technology, India
Naveen Bunekar,
Chung Yuan Christian University, Taiwan

*CORRESPONDENCE
Fahad Alsaikhan,
fsaikhan@hotmail.com

RECEIVED 20 July 2023
ACCEPTED 06 September 2023
PUBLISHED 18 September 2023

CITATION
Alkhathami AG,
Khaled Younis Albahadly W, Jawad MA,
Ramadan MF, Alsaraf KM,
Riyad Muedii ZA-H, Alsaikhan F and
Suliman M (2023), Hydrogel assistant
synthesis of new Ti-MOF cross-linked
oxidized pectin and chitosan with anti-
breast cancer properties.
Front. Mater. 10:1264529.
doi: 10.3389/fmats.2023.1264529

Hydrogel assistant synthesis of new Ti-MOF cross-linked oxidized pectin and chitosan with anti-breast cancer properties

Ali G. Alkhathami[1], Waleed Khaled Younis Albahadly[2], Mohammed Abed Jawad[3], Montather F. Ramadan[4], Khulood Majid Alsaraf[5], Zainab Al-Hawraa Riyad Muedii[6], Fahad Alsaikhan[7]* and Muath Suliman[1]

[1]Department of Clinical Laboratory Sciences, College of Applied Medical Sciences, King Khalid University, Abha, Saudi Arabia, [2]College of Pharmacy, University of Al-Ameed, Karbala, Iraq, [3]Department of Anesthesia, Al-Nisour University College, Baghdad, Iraq, [4]College of Dentistry, Al-Ayen University, Thi-Qar, Iraq, [5]College of Pharmacy, Al-Esraa University College, Baghdad, Iraq, [6]College of Pharmacy, National University of Science and Technology, Dhi Qar, Iraq, [7]College of Pharmacy, Prince Sattam Bin Abdulaziz University, Alkharj, Saudi Arabia

Breast cancer is one of the most common diseases of the modern age. Although many methods for its treatment have been reported so far, the report and synthesis of new compounds based on new technologies, especially nanotechnology, is important. One of the laboratory methods for evaluating the anticancer properties of compounds is the *in vitro* MTT method (3-(4,5-Dimethylthiazol-2-yl)-2,5-Diphenyltetrazolium Bromide). In this study, the *in vitro* anti-breast cancer activity of the newly synthesized (Titanium Metal-Organic Framework) Ti-MOF cross-linked oxidized pectin and chitosan hydrogel, which uses biopolymers in its synthesis and structure, was investigated. The anticancer activity results showed that the synthetic nanopolymer had cell proliferation and viability of 27% more than the control and (the half maximal inhibitory concentration) IC_{50} of 111 µg/mL against breast cancer cells. Before the anticancer evaluation, the structure of the synthesized Ti-MOF cross-linked oxidized pectin, and chitosan hydrogel was confirmed by (X-Ray Diffraction) XRD pattern (Fourier Transform Infrared) FT-IR spectrum (Energy-dispersive X-ray) EDAX spectroscopy, N_2 adsorption/desorption isotherm and (Scanning Electron Microscope) Scanning Electron Microscope images. The results of identification and characterization showed that the synthetic nanopolymer was in the range of nanoparticles. The peaks of the expected functional groups and reactant elements were observed in the FT-IR spectrum and energy-dispersive X-ray spectroscopy of the final product. High physicochemical capabilities such as the uniform morphology, crystallization of particles, and high specific surface area from synthesized Ti-MOF cross-linked oxidized pectin, and chitosan hydrogel were observed. The unique properties of the synthesized Ti-MOF cross-linked oxidized pectin and chitosan hydrogel can be attributed to the appropriate method of its synthesis that was carried out in this study.

KEYWORDS

breast cancer, MTT method, Ti-MOF, biopolymers, hydrogel

1 Introduction

According to a previous study, the synthesis of nanoparticles with hydrogel assisted method can be produced nanoparticles with uniform morphology and small particle size distribution (Wang et al., 2008; Harish et al., 2023). Crystallization of nanoparticles is another crucial advantage of using the hydrogel method in the synthesis of nanoparticles (Chen et al., 2009; Su et al., 2020; Li L. et al, 2021; Azadbakht et al., 2023). Various bioactive nanostructures, including metal oxides, nano complexes and metal-organic frameworks (MOFs), *etc.*, can be synthesized by the hydrogel method (Akbari et al., 2022; Liu Y. et al, 2022; Bustamante-Torres et al., 2022; Oderinde et al., 2022; Li et al., 2023; Lim et al., 2023). The MOFs are an essential group of nanostructures whose unique physical and chemical properties, such as high heat stability, high porosity, *etc.* These unique properties have led to an increase in their reactivity and have attracted the attention of scientists in various fields. Industrial applications such as electrochemical energy conversion and storage, the removal of toxic dyes, adsorbents, and catalysts in the removal of persistent organic pollutants, *etc.*, have been reported so far from these nanostructures (Peng et al., 2022; Sriram et al., 2022; Naghdi et al., 2023). In addition, biomedical applications such as enzyme immobilization, drug delivery, antimicrobial activity, anticancer activity, *etc.*, have been reported from MOFs compounds (Alavijeh and Akhbari, 2022; Han et al., 2022; Maranescu and Visa, 2022; Silva et al., 2022; Guo et al., 2023). In the synthesis of MOF, various metals, such as copper, cobalt, titanium, *etc.*, can be used and synthesized, and depending on the metal used, MOFs have different properties (Liu P. et al, 2022; Fan and Tahir, 2022; Pan et al., 2022). As you know, metal is a significant part of the MOF compounds, which can diversify the hybridization states by varying the oxidation number (Guan and Han, 2019). The titanium is not only effective in hybridization and formation of MOF nanostructures, but also has anti-corrosion properties (Zhang et al., 2021), wear resistance (Bai et al., 2021) and desirable physicochemical properties. As mentioned, MOFs containing titanium have been synthesized so far, and there have been reports of photocatalytic activity, antimicrobial activity, and anticancer activity of Ti-MOFs (Abdelhameed et al., 2022; Kar et al., 2022; Abdelhameed et al., 2023). Advanced nanostructures containing polymer compounds and Ti-MOFs, such as potassium poly (heptazine imide)/Ti-based metal-organic framework composites, have been reported (Rodríguez et al., 2017). Nowadays, the use of polymers in our daily life is unavoidable. Polymers are used in various compounds and industries. In addition, the structure of many vital body compounds and natural compounds such as DNA, starch, cellulose, pectin, and chitosan are also polymeric. Pectin is a robust fiber found naturally in many plants and vegetables (Sila et al., 2009). There have been several reports on using pectin in the structure of synthesized catalysts to synthesize organic compounds and heterocyclic compounds (Dohendou et al., 2021; Khashei Siuki et al., 2022). Pharmacological applications and bioactive compounds containing pectin have been synthesized and reported (Minzanova et al., 2018; Devasvaran and Lim, 2021). According to one of the recent reports, composite films containing pectin derivatives and chitosan have been synthesized with blood compatibility and antibacterial activity (Chetouani et al., 2017). Chitosan is another natural polymer compound that has many capabilities. This polymer, which is abundantly found in the exoskeleton of arthropods such as shrimp, crab, yeast, and insect cuticle, is a biodegradable, biocompatible, and non-toxic polymer that has many biomedical applications (Pakdel and Peighambardoust, 2018; Tapdiqov, 2020; Li D.-q. et al, 2021). Polymeric structures with numerous and remarkable properties of chitosan have been reported. For example, super hydrophobic chitosan-based derived coatings have been reported in 2022 (Roy et al., 2022). Polymers containing chitosan, pectin, and Ti-MOF can have unique biological capabilities, and in this study, using the hydrogel method, we synthesized a new polymer containing them. After identifying and confirming the structure of synthesized Ti-MOF cross-linked oxidized pectin and chitosan by the MTT method, the anticancer properties of breast cancer cells were investigated in different concentrations, treatment time, and various parameters such as IC_{50} and cell proliferation and viability were reported.

2 Material and methods

2.1 Materials

All solvents and raw materials used for the synthesis of compounds such as Titanium (IV) nitrate tetrahydrate (Sigma-Aldrich, 295.89 g mol^{-1}, 99.9%), 2, 6- pyridine dicarboxylic acid (Sigma-Aldrich, MW 167.12 g mol^{-1}, 99%), Chitosan (Sigma-Aldrich, 10 mg/mL acetic acid: water) and Pectin (Pectin from citrus peel, impurities ≤10% moisture, Sigma-Aldrich) were obtained from Merck and Sigma-Aldrich companies with high purity. MCF-7 breast cancer cells (ATCC HTB-22) were prepared from the American Type Culture Collection.

2.2 Devices

By using Bruker Tensor 27 FT-IR, FT-IR spectra of synthesized compounds were prepared. The XRD patterns of synthesized nanostructure by using Bruker D8 X-ray diffractometer were obtained. The SEM images of synthetic compounds were obtained using Hitachi S-4800 FESEM. The N_2 adsorption/desorption of synthesized nanostructure by using Micromeritics ASAP 2460 was prepared.

2.3 Synthesis of Ti-MOF

A mixture of 0.1 mmol Titanium (IV) nitrate tetrahydrate and 0.1 mmol 2, 6- pyridine dicarboxylic acid in 25 mL double-distilled water were placed in an ultrasonic bath with power of 150 W in 30°C for 20 min. Finally, the synthesized Ti-MOF, after separation, was washed three times with a mixture of water and ethanol and dried at 25 C for 48 h (Scheme 1).

2.4 Synthesis of Ti-MOF cross-linked oxidized pectin and chitosan hydrogel

For the synthesis of Ti-MOF cross-linked oxidized pectin and chitosan hydrogel (Figure 1), a previously reported protocol was used (Salama and Aziz, 2020). At first, 0.1 mmol of oxidized pectin

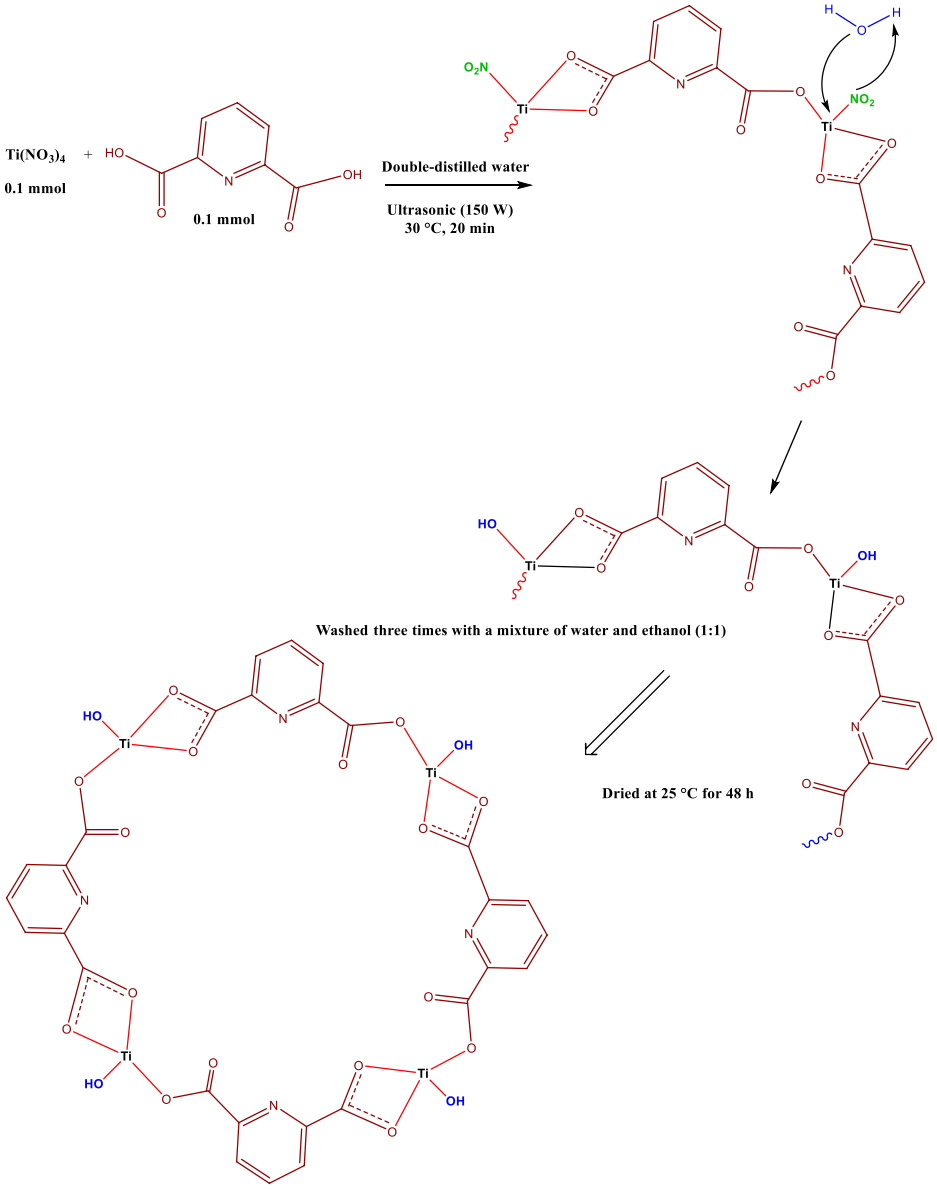

SCHEME 1
Proposed mechanism for synthesis Ti-MOF

were dissolved in 10 mL of double-distilled water under stirring at 30°C. In different containers, 0.2 mmol of chitosan were dispersed in 20 mL of double-distilled water using ultrasonic at 30°C. Then 0.1 mmol of Ti-MOF was added to the container containing oxidized pectin and stirred for 1 h at the same temperature with a speed of 800 rpm. Then, the mixture containing chitosan was added drop by drop to the container containing oxidized pectin and Ti-MOF. After that, the mixture was stirred at the same temperature for 1 h under the previous temperature conditions. Finally, the resulting mixture was placed in a water bath at 37°C for 4 h (Scheme 2).

The synthesis procedure of oxidized pectin developed in this study was reported based on previous literature. In 75 mL EtOH, 0.5 mmol g of Pectin was dispersed. Then, at dark and room temperature, sodium periodate solution (0.15 mmol/50 mL) dropwise was added. The mixture was stirred for 2 h at room temperature, and added ethylene glycol to the oxidation reaction to be terminated. By centrifuging at 6000 rpm, the supernatant layer was collected, and synthesized Oxidized pectin was kept in a dialysis bag for 3 days to be freeze-dried (Nejati et al., 2020).

2.5 Anti-breast cancer cells activity of Ti-MOF cross-linked oxidized pectin and chitosan

In the control medium containing RPMI (Roswell Park Memorial Institute) 1640, 10% FBS (Fetal Bovine Serum), and penicillin G/streptomycin (200 µL), MCF-7 breast cancer cells were cultured. In microplates, 200 µL MCF-7 breast cancer cells

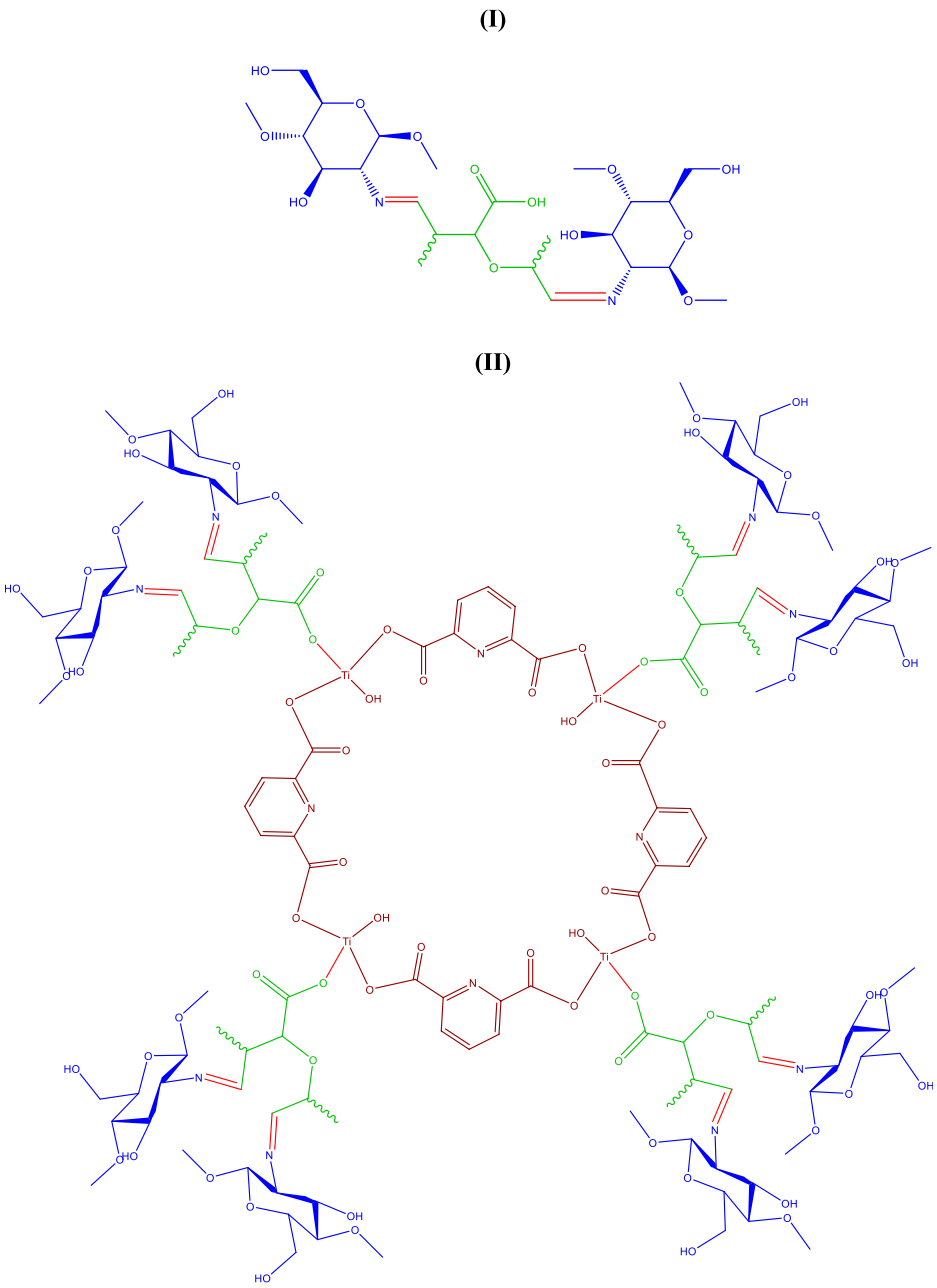

FIGURE 1
Proposed structure for oxidized pectin-chitosan hydrogel (I) Ti-MOF cross-linked oxidized pectin and chitosan hydrogel (II).

with a density of 1.2×10^4 cells per well were seeded and, in conditions of 5% CO_2 and 37°C for 24 h, were incubated. Concentrations of 5, 10, 20, 40, 80, 120, and 200 mg/μL from Ti-MOF cross-linked oxidized pectin were added to each well, and were treated for 24 and 48 h under conditions of 5% CO_2 and 37°C. A solution of 2 μg/mL MTT was prepared in PBS. After the stated time (24 and 48 h), the medium containing Ti-MOF cross-linked oxidized pectin and chitosan were removed, and 50 μL of prepared MTT solution and 150 μL of fresh medium were added to the wells and placed in the incubator under conditions of 5% CO_2 and 37°C for 4 h. Then the medium containing MTT was removed, and 200 μL of dimethyl sulfoxide was added to the wells. The absorbance at 570 nm was read by an ELISA (Anzyme-Linked Immuno Sorbent Assay) reader (Heidari Majd et al., 2017).

3 Result and discussion

3.1 Result and characterization of Ti-MOF cross-linked oxidized pectin and chitosan hydrogel

From the complexation of Ti-MOF with oxidized pectin and finally using the Schiff base reaction of Ti-MOF-oxidized pectin

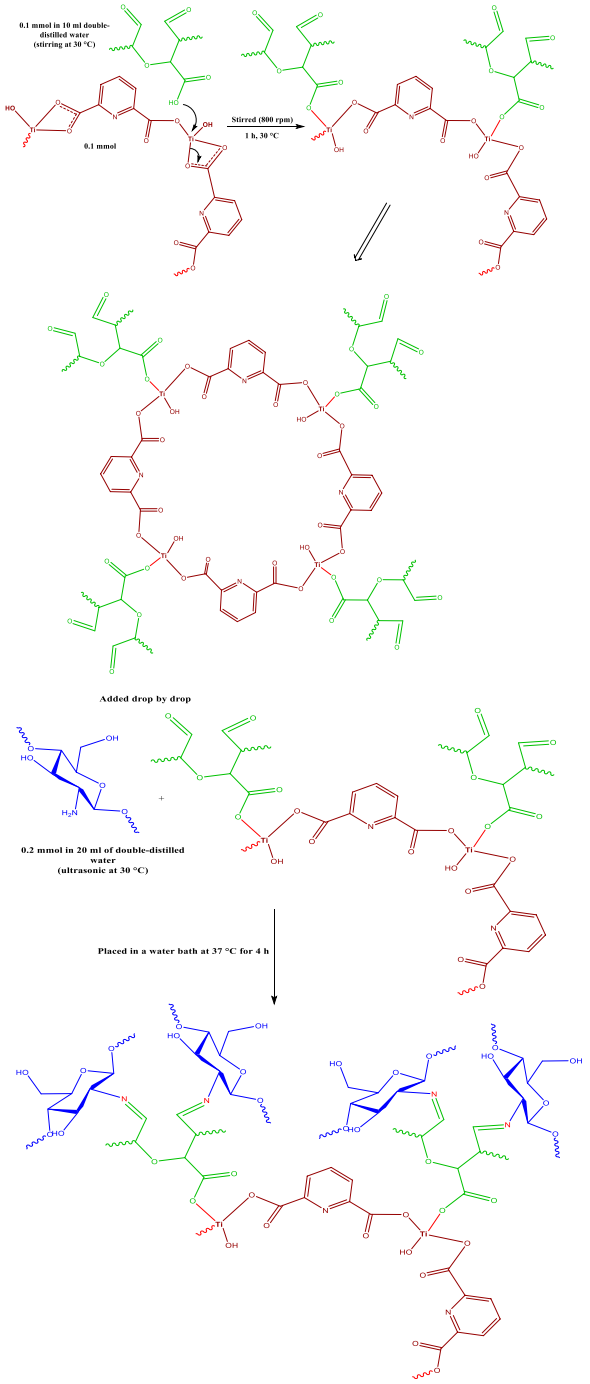

SCHEME 2
Proposed mechanism for synthesis Ti-MOF cross-linked oxidized pectin and chitosan hydrogel

complex with chitosan, novel Ti-MOF cross-linked oxidized pectin and chitosan hydrogel was synthesized.

First, by using Titanium (IV) nitrate tetrahydrate and 2, 6-pyridine dicarboxylic acid under ultrasonic conditions, Ti-MOF was synthesized (Scheme 1). By adding Ti-MOF to the oxidized pectin solution, Ti-MOF containing oxidized pectin was synthesized. Finally, by adding a mixture containing chitosan to Ti-MOF/oxidized pectin and performing the Schiff base reaction, Ti-MOF cross-linked oxidized pectin, and chitosan hydrogel were synthesized (Scheme 1).

The structure of Figure 1 is proposed for the new synthesized Ti-MOF cross-linked oxidized pectin and chitosan hydrogel, which was identified and confirmed by spectral data and analyses of XRD (X-Ray Diffraction pattern, and FT-IR (Fourier Transform Infrared spectrum, EDAX (Energy-dispersive X-ray) spectroscopy, N_2 adsorption/desorption isotherm and SEM (Scanning Electron Microscope) images.

Figure 2 shows the XRD patterns (A) and FT-IR spectrums (B) of synthesized Ti-MOF (I) and Ti-MOF cross-linked oxidized pectin and chitosan hydrogel (II). As can be seen in XRD patterns (Figure 2A), based on previous reports, the peaks related to the crystal structure of titanium nanoparticles were observed in the XRD pattern of Ti-MOF and Ti-MOF cross-linked oxidized pectin and chitosan hydrogel. In the XRD patterns (I) and (II), plates corresponding to Ti nanostructures ([011], [002], [121], [222], and [132]) were obverted (Hacisalihoglu et al., 2015; Han et al., 2015; Gómez-Avilés et al., 2020).

Using XRD patterns and the Debye-Scherer equation, the mean crystalline size of Ti-MOF and Ti-MOF cross-linked oxidized pectin and chitosan hydrogel was calculated and found to be 52 and 67 nm, respectively. As a signicant result, it can be stated that the synthesis method in this study had a good effect on the crystallization and nanosizing of the synthesized Ti-MOF and Ti-MOF cross-linked oxidized pectin and chitosan hydrogel.

In the FT-IR spectra of Ti-MOF (Figure 2B-I) and Ti-MOF cross-linked oxidized pectin and chitosan hydrogel (Figure 2B-II), as seen in Figure 2B, the peaks related to the links and functional groups of the proposed structure of the desired product are observed. For example, the peak related to Ti-O near 650 cm^{-1} was observed (Al-Amin et al., 2016). Peaks related to groups C-O, C=C, C=N, and C=O were observed in areas 1,100, 1,400, 1,500, and 1,600 cm^{-1}, respectively (Bakhshi et al., 2022). One of the most important peaks that represent the synthesis of Ti-MOF cross-linked oxidized pectin and chitosan hydrogel based on the proposed structure is C-H peaks, as seen in Figure 2B-II. These peaks are observed in the region below 3,000 cm^{-1}. The peak related to the OH group was also observed in the areas above 3,000 cm^{-1}.

Energy-dispersive X-ray spectroscopy and the elemental analysis related to the final product (Ti-MOF cross-linked oxidized pectin and chitosan hydrogel) are shown in Figure 3 and Table 1. As shown in Figure 3, the raw material elements are present in the structure of the proposed final product. The elemental analysis results next to Energy-dispersive X-ray spectroscopy prove the formation of the proposed compound. As an important result, elemental analyses confirmed the successful synthesis of Ti-MOF and Ti-MOF cross-linked oxidized pectin.

The curves of N_2 adsorption/desorption isotherm of Ti-MOF (I) and Ti-MOF cross-linked oxidized pectin and chitosan hydrogel (II) are given in Figure 4. The specific surface area for Ti-MOF (I) and Ti-MOF cross-linked oxidized pectin and chitosan hydrogel (II), based on the results of BET, was obtained about 28 and 34 m^2/g, respectively. According to the IUPAC classification of adsorption/desorption isotherm, the behavior of both samples is similar to the second type of isotherms, which confirms the macroporous size distribution for Ti-MOF and Ti-MOF cross-linked oxidized pectin and chitosan hydrogel (Sargazi et al., 2018). The significant porosity

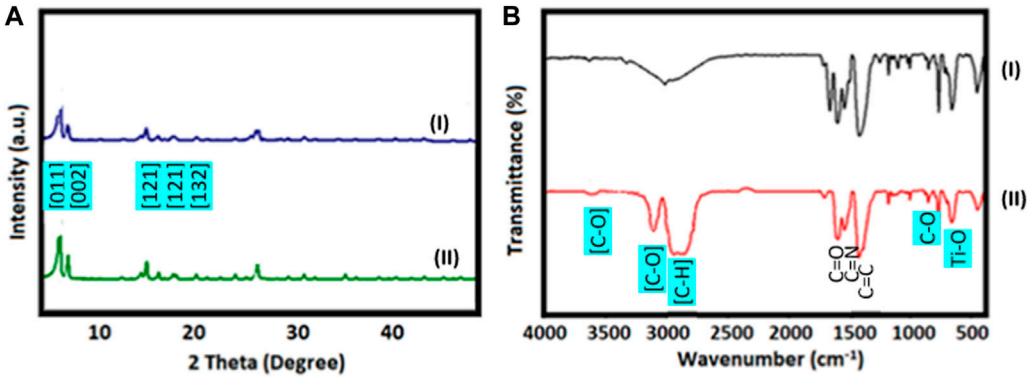

FIGURE 2
XRD patterns **(A)** and FT-IR spectrums **(B)** of Ti-MOF (I) and Ti-MOF cross-linked oxidized pectin and chitosan hydrogel (II).

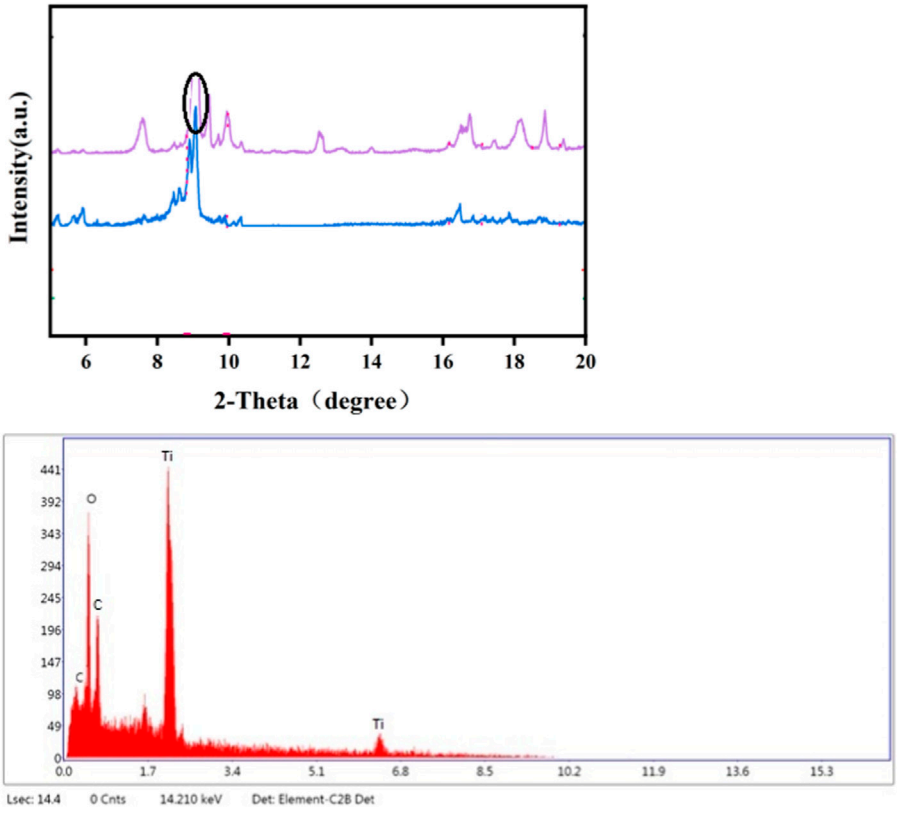

FIGURE 3
EDAX spectroscopy of Ti-MOF cross-linked oxidized pectin and chitosan hydrogel.

of the products provides good potential for diverse applications of these novel materials. The results proved that the polymerization of Ti-MOF with oxidized pectin and chitosan increases its specific surface area. As we know, the high specific surface area in nanoparticles makes compounds highly effective in biological fields and their catalytic applications. On the other hand, the specific surface area is highly dependent on the synthesis method of nanoparticles. Therefore, the synthesis methods in this study are suitable for synthesizing the desired products and have increased the specific surface area of the synthetic compounds.

The scanning electron microscope images related to Ti-MOF (I) and Ti-MOF cross-linked oxidized pectin and chitosan hydrogel are shown in Figure 5. The images show the nanosize structure, uniform morphology, and good crystallinity. According to the SEM image, the Ti-MOF nanostructure has homogeneous morphology with nanosized distribution. Compared to Ti-MOF, Ti-MOF cross-

TABLE 1 Elemental analysis of Ti-MOF cross-linked oxidized pectin and chitosan hydrogel.

Element	C	H	N	O
Actual	45.17	5.64	5.26	36.31
Theoretical	46.80	5.70	5.28	36.20

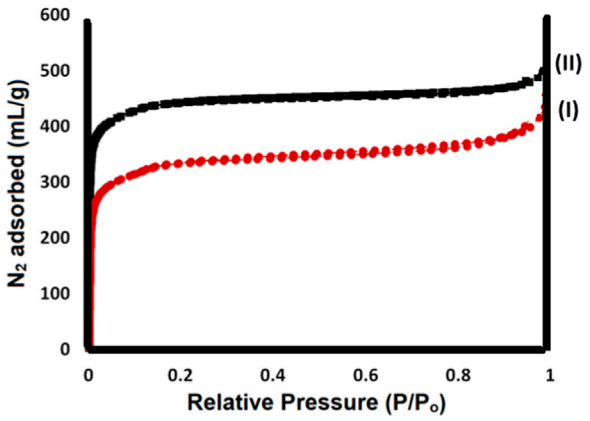

FIGURE 4
N_2 adsorption/desorption isotherm of Ti-MOF (I) and Ti-MOF cross-linked oxidized pectin and chitosan hydrogel (II).

linked oxidized pectin, and chitosan hydrogel tend to aggregate in final structures, slightly. It can be related to the efficient loading of the linkers in Ti-MOF nanostructures. Also, the acceptance stability of Ti-MOF cross-linked oxidized pectin in final products can be related to the efficient synthesis method of nanoparticles. As mentioned in the previous parts, the synthesis method has caused the above characteristics to the synthesized nanoparticles of this study (Sargazi et al., 2019; Moghaddam-manesh et al., 2022).

As a general result, it can be said that the ultrasonic and hydrogel method used in this study is an effective method for the synthesis of Ti-MOF and Ti-MOF cross-linked oxidized pectin and chitosan hydrogel, with high physicochemical capabilities such as nano-size and uniform morphology, crystallization of particles and high specific surface area.

3.2 Result of anti-breast cancer cells activity of Ti-MOF cross-linked oxidized pectin and chitosan hydrogel

Based on the MTT method, the anti-breast cancer cell activity of Ti-MOF cross-linked oxidized pectin and chitosan was studied based on the MTT method. For this purpose, breast cancer cells were treated with various concentrations of Ti-MOF cross-linked oxidized pectin and chitosan. In addition to different concentrations, studies were evaluated at 24 and 48 h. The results of the investigations are given in the curves of Figure 6 and Figure 7.

As seen in Figure 6 and Figure 7, the highest cell proliferation and viability of Ti-MOF cross-linked oxidized pectin and chitosan is at a concentration of 200 mg/mL at 24 and 48 h. The cell proliferation and viability at 200 µg/mL of Ti-MOF cross-linked oxidized pectin and chitosan in 24 h were 33.68% more than the control, and in 48 h,27% more than the control were observed.

From the results of the observed values, it can be concluded that the effect on breast cancer cells depends on the concentration of Ti-MOF cross-linked oxidized pectin and chitosan and treatment time.

The IC_{50} (The half maximal inhibitory concentration) values for 24 and 48 h, using the equation of the line that was obtained from the curve of concentration and cell proliferation and viability in different concentrations, were calculated as 137 and 111 µg/mL, respectively.

The effectiveness of nanoparticles on breast cancer cells can be attributed to factors such as the porous and specific surface area of Ti-MOF, the presence of titanium as bioactive metal, and the bioactive polymers, including chitosan and oxidized pectin, that are present in the structure of newly synthesized polymer (Leclere

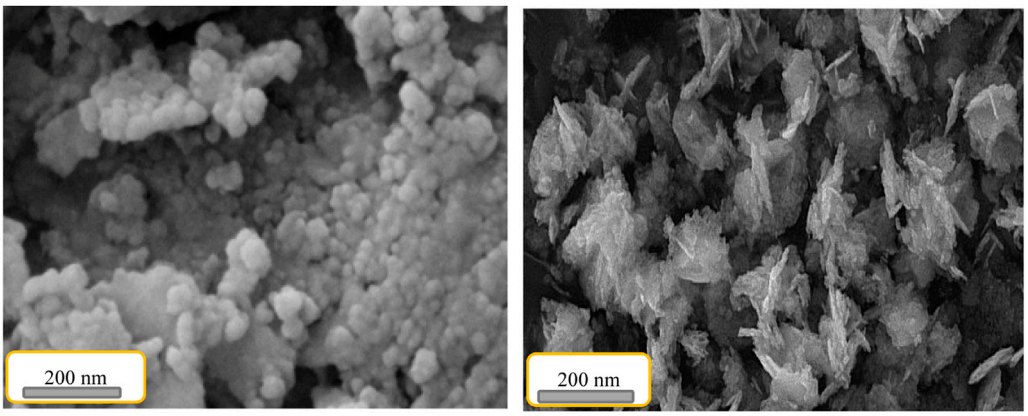

FIGURE 5
Scanning electron microscope images of Ti-MOF (I) and Ti-MOF cross-linked oxidized pectin and chitosan hydrogel (II).

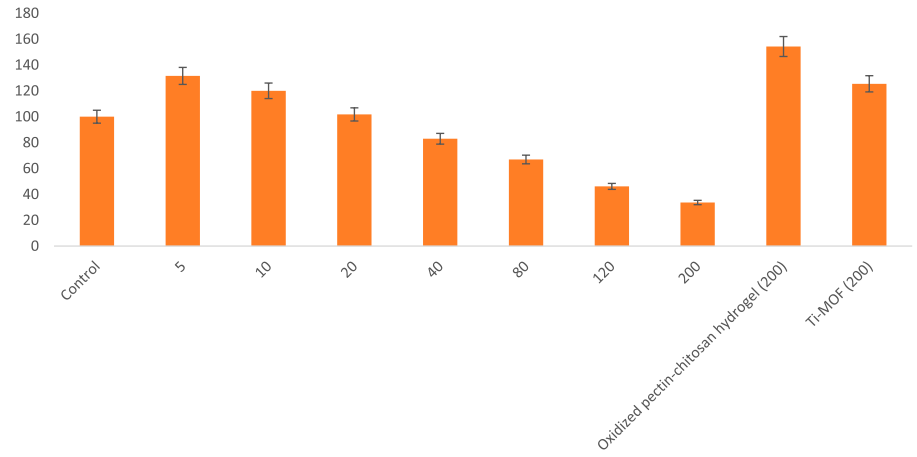

FIGURE 6
The cell proliferation and viability of Ti-MOF cross-linked oxidized pectin and chitosan hydrogel on breast cancer cells activity at 24 h (mean (n = 3) ± SD).

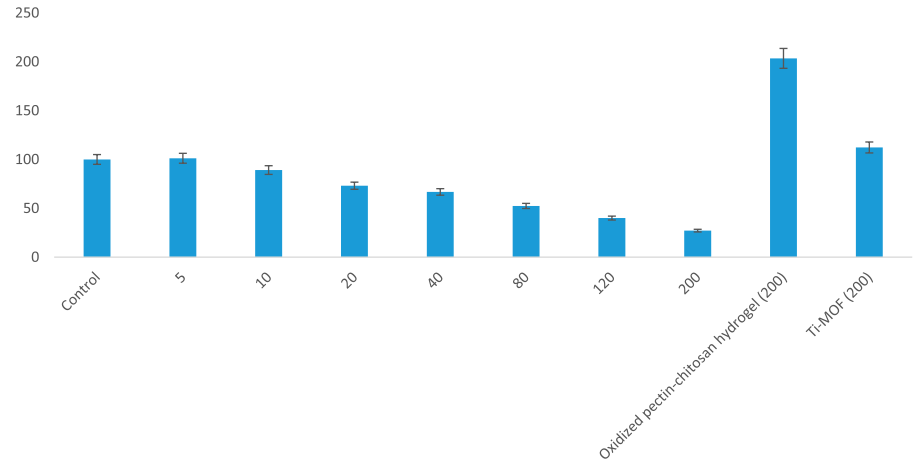

FIGURE 7
The cell proliferation and viability of Ti-MOF cross-linked oxidized pectin and chitosan hydrogel on breast cancer cells activity at 48 h (mean (n = 3) ± SD).

et al., 2013; Wimardhani et al., 2014; Murugan et al., 2016; Adhikari and Yadav, 2018; Aswini et al., 2021; Ali et al., 2022).

4 Conclusion

Ti-MOF cross-linked oxidized pectin and chitosan hydrogel were synthesized as a novel polymeric nanostructure. Prediction and confirmation of the structure of the newly synthesized nanopolymer using XRD pattern, FT-IR spectrum, EDAX spectroscopy, N_2 adsorption/desorption isotherm, and SEM images were done. In examining the structure of the synthesized nanoparticles, high specific surface area, crystallization of particles, and uniform morphology were observed. These unique features can be attributed to the method used in the synthesis. The unique physical and chemical properties of the synthesized Ti-MOF cross-linked oxidized pectin and chitosan hydrogel, especially the high specific surface area, made it highly active in inhibiting breast cancer cells. The MTT method was used to determine the anticancer effects of the synthesized Ti-MOF cross-linked oxidized pectin and chitosan hydrogel, and cell proliferation and viability and IC_{50} values in different concentrations and times of 24 h and 48 h were evaluated and calculated. The highest cell proliferation and viability were observed at a concentration of 200 mg/mL in 48 h at a rate of 27% compared to the control. The best IC_{50} values were calculated at 111 µg/mL in 48 h. Observations proved that the effect on breast cancer cells depends on the concentration of Ti-MOF cross-linked oxidized pectin and chitosan and exposed time.

Data availability statement

The original contributions presented in the study are included in the article/Supplementary Material, further inquiries can be directed to the corresponding author.

Author contributions

AA: Funding acquisition, Writing–review and editing. WK: Supervision, Validation, Writing–original draft. MJ: Resources, Writing–original draft. MR: Investigation, Project administration, Writing–review and editing. KA: Visualization, Writing–original draft. ZA-HR: Methodology, Writing–review and editing. FA: Conceptualization, Validation, Writing–original draft, Writing–review and editing. MS: Formal Analysis, Writing–original draft.

Funding

The authors declare that no financial support was received for the research, authorship, and/or publication of this article.

Acknowledgments

The authors extend their appreciation to the Deanship of Scientific Research at King Khalid University for funding this work through small research program under grant number RGP.2-216-43.

Conflict of interest

The authors declare that the research was conducted in the absence of any commercial or financial relationships that could be construed as a potential conflict of interest.

Publisher's note

All claims expressed in this article are solely those of the authors and do not necessarily represent those of their affiliated organizations, or those of the publisher, the editors and the reviewers. Any product that may be evaluated in this article, or claim that may be made by its manufacturer, is not guaranteed or endorsed by the publisher.

References

Abdelhameed, R. M., Abu-Elghait, M., and El-Shahat, M. (2022). Engineering titanium-organic framework decorated silver molybdate and silver vanadate as antimicrobial, anticancer agents, and photo-induced hydroxylation reactions. *J. Photochem. Photobiol. A Chem.* 423, 113572. doi:10.1016/j.jphotochem.2021.113572

Abdelhameed, R. M., Darwesh, O. M., and El-Shahat, M. (2023). Titanium-based metal-organic framework capsulated with magnetic nanoparticles: antimicrobial and photocatalytic degradation of pesticides. *Microporous Mesoporous Mater.* 354, 112543. doi:10.1016/j.micromeso.2023.112543

Adhikari, H. S., and Yadav, P. N. (2018). Anticancer activity of chitosan, chitosan derivatives, and their mechanism of action. *Int. J. Biomaterials* 2018, 1–29. doi:10.1155/2018/2952085

Akbari, V., Rezazadeh, M., Hanaie, N. S., and Hasanzadeh, F. (2022). Preparation and *in vitro* characterization of histidine trimethyl chitosan conjugated nanocomplex incorporated into injectable thermosensitive hydrogels for localized gene delivery. *Biotechnol. Appl. Biochem.* 69 (3), 1047–1057. doi:10.1002/bab.2175

Al-Amin, M., Dey, S. C., Rashid, T. U., Ashaduzzaman, M., and Shamsuddin, S. M. (2016). Solar assisted photocatalytic degradation of reactive azo dyes in presence of anatase titanium dioxide. *Int. J. Latest Res. Eng. Technol.* 2 (3), 14–21.

Alavijeh, R. K., and Akhbari, K. (2022). Improvement of curcumin loading into a nanoporous functionalized poor hydrolytic stable metal-organic framework for high anticancer activity against human gastric cancer AGS cells. *Colloids Surfaces B Biointerfaces* 212, 112340. doi:10.1016/j.colsurfb.2022.112340

Ali, O. M., Hasanin, M. S., Suleiman, W. B., Helal, E. E.-H., and Hashem, A. H. (2022). Green biosynthesis of titanium dioxide quantum dots using watermelon peel waste: antimicrobial, antioxidant, and anticancer activities. *Biomass Convers. Biorefinery*, 1–12. doi:10.1007/s13399-022-02772-y

Aswini, R., Murugesan, S., and Kannan, K. (2021). Bio-engineered tio2 nanoparticles using ledebouria revoluta extract: larvicidal, histopathological, antibacterial and anticancer activity. *Int. J. Environ. Anal. Chem.* 101 (15), 2926–2936. doi:10.1080/03067319.2020.1718668

Azadbakht, A., Alizadeh, S., Aliakbar Ahovan, Z., Khosrowpour, Z., Majidi, M., Pakzad, S., et al. (2023). Chitosan-placental ECM composite thermos-responsive hydrogel as a biomimetic wound dressing with angiogenic property. *Macromol. Biosci.* 23 (2), 2200386. doi:10.1002/mabi.202200386

Bai, H., Zhong, L., Kang, L., Liu, J., Zhuang, W., Lv, Z., et al. (2021). A review on wear-resistant coating with high hardness and high toughness on the surface of titanium alloy. *J. Alloys Compd.* 882, 160645. doi:10.1016/j.jallcom.2021.160645

Bakhshi, A., Saravani, H., Rezvani, A., Sargazi, G., and Shahbakhsh, M. (2022). A new method of Bi-MOF nanostructures production using UAIM procedure for efficient electrocatalytic oxidation of aminophenol: A controllable systematic study. *J. Appl. Electrochem.* 52, 709–728. doi:10.1007/s10800-021-01664-9

Bustamante-Torres, M., Romero-Fierro, D., Estrella-Nuñez, J., Arcentales-Vera, B., Chichande-Proaño, E., and Bucio, E. (2022). Polymeric composite of magnetite iron oxide nanoparticles and their application in biomedicine: A review. *Polymers* 14 (4), 752. doi:10.3390/polym14040752

Chen, C. H., Abate, A. R., Lee, D., Terentjev, E. M., and Weitz, D. A. (2009). Microfluidic assembly of magnetic hydrogel particles with uniformly anisotropic structure. *Adv. Mater.* 21 (31), 3201–3204. doi:10.1002/adma.200900499

Chetouani, A., Follain, N., Marais, S., Rihouey, C., Elkolli, M., Bounekhel, M., et al. (2017). Physicochemical properties and biological activities of novel blend films using oxidized pectin/chitosan. *Int. J. Biol. Macromol.* 97, 348–356. doi:10.1016/j.ijbiomac.2017.01.018

Devasvaran, K., and Lim, V. (2021). Green synthesis of metallic nanoparticles using pectin as a reducing agent: A systematic review of the biological activities. *Pharm. Biol.* 59 (1), 492–501. doi:10.1080/13880209.2021.1910716

Dohendou, M., Pakzad, K., Nezafat, Z., Nasrollahzadeh, M., and Dekamin, M. G. (2021). Progresses in chitin, chitosan, starch, cellulose, pectin, alginate, gelatin and gum based (nano) catalysts for the Heck coupling reactions: A review. *Int. J. Biol. Macromol.* 192, 771–819. doi:10.1016/j.ijbiomac.2021.09.162

Fan, W. K., and Tahir, M. (2022). Recent advances on cobalt metal organic frameworks (MOFs) for photocatalytic CO2 reduction to renewable energy and fuels: A review on current progress and future directions. *Energy Convers. Manag.* 253, 115180. doi:10.1016/j.enconman.2021.115180

Gómez-Avilés, A., Muelas-Ramos, V., Bedia, J., Rodriguez, J. J., and Belver, C. (2020). Thermal post-treatments to enhance the water stability of NH2-MIL-125 (Ti). *Catalysts* 10 (6), 603. doi:10.3390/catal10060603

Guan, G., and Han, M. Y. (2019). Functionalized hybridization of 2D nanomaterials. *Adv. Sci.* 6 (23), 1901837. doi:10.1002/advs.201901837

Guo, W., Gao, W., Li, Q., Qu, S., Zhang, L., Tan, L.-L., et al. (2023). Plasmon-enhanced visible-light photocatalytic antibacterial activity of metal-organic framework/gold nanocomposites. *J. Mater. Chem. A* 11, 2391–2401. doi:10.1039/d2ta09061a

Hacisalihoglu, I., Samancioglu, A., Yildiz, F., Purcek, G., and Alsaran, A. (2015). Tribocorrosion properties of different type titanium alloys in simulated body fluid. *Wear* 332, 679–686. doi:10.1016/j.wear.2014.12.017

Han, I., Choi, S. A., and Lee, D. N. (2022). Therapeutic application of metal–organic frameworks composed of copper, cobalt, and zinc: their anticancer activity and mechanism. *Pharmaceutics* 14 (2), 378. doi:10.3390/pharmaceutics14020378

Han, M.-K., Im, J.-B., Hwang, M.-J., Kim, B.-J., Kim, H.-Y., and Park, Y.-J. (2015). Effect of indium content on the microstructure, mechanical properties and corrosion behavior of titanium alloys. *Metals* 5 (2), 850–862. doi:10.3390/met5020850

Harish, V., Ansari, M., Tewari, D., Yadav, A. B., Sharma, N., Bawarig, S., et al. (2023). Cutting-edge advances in tailoring size, shape, and functionality of nanoparticles and nanostructures: A review. *J. Taiwan Inst. Chem. Eng.* 149, 105010. doi:10.1016/j.jtice.2023.105010

Heidari Majd, M., Akbarzadeh, A., and Sargazi, A. (2017). Evaluation of host–guest system to enhance the tamoxifen efficiency. *Artif. cells, nanomedicine, Biotechnol.* 45 (3), 441–447. doi:10.3109/21691401.2016.1160916

Kar, A. K., Behera, A., and Srivastava, R. (2022). Pd-Embedded Ti metal–organic framework nanostructures for photocatalytic reductive N-Formylation of nitroarenes in water. *Acs Appl Nano Mater.* 5 (1), 464–475. doi:10.1021/acsanm.1c03310

Khashei Siuki, H., Ghamari Kargar, P., and Bagherzade, G. (2022). New acetamidine Cu (II) Schiff base complex supported on magnetic nanoparticles pectin for the synthesis of triazoles using click chemistry. *Sci. Rep.* 12 (1), 3771. doi:10.1038/s41598-022-07674-7

Leclere, L., Cutsem, P. V., and Michiels, C. (2013). Anti-cancer activities of pH-or heat-modified pectin. *Front. Pharmacol.* 4, 128. doi:10.3389/fphar.2013.00128

Li, C., Wang, J., Niu, Y., Zhang, H., Ouyang, H., Zhang, G., et al. (2023). Baicalin nanocomplexes with an in situ-forming biomimetic gel implant for repair of calvarial bone defects via localized sclerostin inhibition. *ACS Appl. Mater. Interfaces.* 15 (7), 9044–9057. doi:10.1021/acsami.2c20946

Li, D. Q., Li, J., Dong, H.-L., Li, X., Zhang, J. Q., Ramaswamy, S., et al. (2021a). Pectin in biomedical and drug delivery applications: A review. *Int. J. Biol. Macromol.* 185, 49–65. doi:10.1016/j.ijbiomac.2021.06.088

Li, L., He, N., Jiang, B., Yu, K., Zhang, Q., Zhang, H., et al. (2021b). Highly salt-resistant 3D hydrogel evaporator for continuous solar desalination via localized crystallization. *Adv. Funct. Mater.* 31 (43), 2104380. doi:10.1002/adfm.202104380

Lim, J. Y., Goh, L., Otake, K.-i., Goh, S. S., Loh, X. J., and Kitagawa, S. (2023). Biomedically-relevant metal organic framework-hydrogel composites. *Biomaterials Sci.* 11, 2661–2677. doi:10.1039/d2bm01906j

Liu, P., Wang, Y., Chen, Y., Wang, X., Yang, J., Li, L., et al. (2022a). Stable titanium metal-organic framework with strong binding affinity for ethane removal. *Chin. J. Chem. Eng.* 42, 35–41. doi:10.1016/j.cjche.2021.07.027

Liu, Y., Huo, Y., Li, M., Qin, C., and Liu, H. (2022b). Synthesis of metal–organic-frameworks on polydopamine modified cellulose nanofibril hydrogels: constructing versatile vehicles for hydrophobic drug delivery. *Cellulose* 29, 379–393. doi:10.1007/s10570-021-04267-x

Maranescu, B., and Visa, A. (2022). Applications of metal-organic frameworks as drug delivery systems. *Int. J. Mol. Sci.* 23 (8), 4458. doi:10.3390/ijms23084458

Minzanova, S. T., Mironov, V. F., Arkhipova, D. M., Khabibullina, A. V., Mironova, L. G., Zakirova, Y. M., et al. (2018). Biological activity and pharmacological application of pectic polysaccharides: A review. *Polymers* 10 (12), 1407. doi:10.3390/polym10121407

Moghaddam-manesh, M., Sargazi, G., Roohani, M., Zanjani, N. G., Khaleghi, M., and Hosseinzadegan, S. (2022). Synthesis of PVA/Fe3O4@ SiO2@ CPS@ SID@ Ni as novel magnetic fibrous composite polymer nanostructures and evaluation of anti-cancer and antimicrobial activity. *Polym. Bull.*, 1–12. doi:10.1007/s00289-022-04584-6

Murugan, K., Dinesh, D., Kavithaa, K., Paulpandi, M., Ponraj, T., Alsalhi, M. S., et al. (2016). Hydrothermal synthesis of titanium dioxide nanoparticles: mosquitocidal potential and anticancer activity on human breast cancer cells (mcf-7). *Parasitol. Res.* 115, 1085–1096. doi:10.1007/s00436-015-4838-8

Naghdi, S., Shahrestani, M. M., Zendehbad, M., Djahaniani, H., Kazemian, H., and Eder, D. (2023). Recent advances in application of metal-organic frameworks (MOFs) as adsorbent and catalyst in removal of persistent organic pollutants (POPs). *J. Hazard. Mater.* 442, 130127. doi:10.1016/j.jhazmat.2022.130127

Nejati, S., Soflou, R. K., Khorshidi, S., and Karkhaneh, A. (2020). Development of an oxygen-releasing electroconductive *in-situ* crosslinkable hydrogel based on oxidized pectin and grafted gelatin for tissue engineering applications. *Colloids Surfaces B Biointerfaces* 196, 111347. doi:10.1016/j.colsurfb.2020.111347

Oderinde, O., Ejeromedoghene, O., and Fu, G. (2022). Synthesis and properties of low-cost, photochromic transparent hydrogel based on ethaline-assisted binary tungsten oxide-molybdenum oxide nanocomposite for optical memory applications. *Polym. Adv. Technol.* 33 (3), 687–699. doi:10.1002/pat.5400

Pakdel, P. M., and Peighambardoust, S. J. (2018). Review on recent progress in chitosan-based hydrogels for wastewater treatment application. *Carbohydr. Polym.* 201, 264–279. doi:10.1016/j.carbpol.2018.08.070

Pan, Q., Xie, L., Liu, R., Pu, Y., Wu, D., Gao, W., et al. (2022). Two birds with one stone: copper metal-organic framework as a carrier of disulfiram prodrug for cancer therapy. *Int. J. Pharm.* 612, 121351. doi:10.1016/j.ijpharm.2021.121351

Peng, Y., Bai, Y., Liu, C., Cao, S., Kong, Q., and Pang, H. (2022). Applications of metal–organic framework-derived N, P, S doped materials in electrochemical energy conversion and storage. *Coord. Chem. Rev.* 466, 214602. doi:10.1016/j.ccr.2022.214602

Rodríguez, N. A., Savateev, A., Grela, M. A., and Dontsova, D. (2017). Facile synthesis of potassium poly (heptazine imide)(PHIK)/Ti-based metal–organic framework (MIL-125-NH2) composites for photocatalytic applications. *ACS Appl. Mater. Interfaces* 9 (27), 22941–22949. doi:10.1021/acsami.7b04745

Roy, S., Goh, K.-L., Verma, C., Dasgupta Ghosh, B., Sharma, K., and Maji, P. K. (2022). A facile method for processing durable and sustainable superhydrophobic chitosan-based coatings derived from waste crab shell. *ACS Sustain. Chem. Eng.* 10 (14), 4694–4704. doi:10.1021/acssuschemeng.2c00206

Salama, H. E., and Aziz, M. S. A. (2020). Novel biocompatible and antimicrobial supramolecular O-carboxymethyl chitosan biguanidine/zinc physical hydrogels. *Int. J. Biol. Macromol.* 163, 649–656. doi:10.1016/j.ijbiomac.2020.07.029

Sargazi, G., Afzali, D., and Mostafavi, A. (2018). An efficient and controllable ultrasonic-assisted microwave route for flower-like ta (v)–mof nanostructures: preparation, fractional factorial design, dft calculations, and high-performance n 2 adsorption. *J. Porous Mater.* 25, 1723–1741. doi:10.1007/s10934-018-0586-3

Sargazi, G., Ebrahimi, A. K., Afzali, D., Badoei-dalfard, A., Malekabadi, S., and Karami, Z. (2019). Fabrication of pva/zno fibrous composite polymer as a novel sorbent for arsenic removal: design and a systematic study. *Polym. Bull.* 76 (11), 5661–5682. doi:10.1007/s00289-019-02677-3

Sila, D., Van Buggenhout, S., Duvetter, T., Fraeye, I., De Roeck, A., Van Loey, A., et al. (2009). Pectins in processed fruits and vegetables: part ii—structure–function relationships. *Compr. Rev. food Sci. food Saf.* 8 (2), 86–104. doi:10.1111/j.1541-4337.2009.00071.x

Silva, A. R., Alexandre, J. Y., Souza, J. E., Neto, J. G. L., de Sousa Júnior, P. G., Rocha, M. V., et al. (2022). The chemistry and applications of metal–organic frameworks (MOFs) as industrial enzyme immobilization systems. *Molecules* 27 (14), 4529. doi:10.3390/molecules27144529

Sriram, G., Bendre, A., Mariappan, E., Altalhi, T., Kigga, M., Ching, Y. C., et al. (2022). Recent trends in the application of metal-organic frameworks (MOFs) for the removal of toxic dyes and their removal mechanism-a review. *Sustain. Mater. Technol.* 31, e00378. doi:10.1016/j.susmat.2021.e00378

Su, Z., He, J., Zhou, P., Huang, L., and Zhou, J. (2020). A high-throughput system combining microfluidic hydrogel droplets with deep learning for screening the antisolvent-crystallization conditions of active pharmaceutical ingredients. *Lab a Chip* 20 (11), 1907–1916. doi:10.1039/d0lc00153h

Tapdiqov, S. Z. (2020). A drug-loaded gel based on graft radical co-polymerization of n-vinylpyrrolidone and 4-vinylpyridine with chitosan. *Cellul. Chem. Technol.* 54, 429–438. doi:10.35812/cellulosechemtechnol.2020.54.44

Wang, Y., Li, B., Zhou, Y., and Jia, D. (2008). Chitosan-induced synthesis of magnetite nanoparticles via iron ions assembly. *Polym. Adv. Technol.* 19 (9), 1256–1261. doi:10.1002/pat.1121

Wimardhani, Y. S., Suniarti, D. F., Freisleben, H. J., Wanandi, S. I., Siregar, N. C., and Ikeda, M.-A. (2014). Chitosan exerts anticancer activity through induction of apoptosis and cell cycle arrest in oral cancer cells. *J. oral Sci.* 56 (2), 119–126. doi:10.2334/josnusd.56.119

Zhang, Z., Zhang, Y., Zhang, S., Yao, K., Sun, Y., Liu, Y., et al. (2021). Synthesis of rare Earth doped MOF base coating on TiO2 nanotubes arrays by electrochemical method using as antibacterial implant material. *Inorg. Chem. Commun.* 127, 108484. doi:10.1016/j.inoche.2021.108484